Identification of Catalytic Bases in the Active Site of *Escherichia coli* Methylglyoxal Synthase: Cloning, Expression, and Functional Characterization of Conserved Aspartic Acid Residues†

Dana Saadat and David H. T. Harrison*

Department of Biochemistry, Medical College of Wisconsin, 8701 Watertown Plank Rd., Milwaukee, Wisconsin 53226

Received February 20, 1998; Revised Manuscript Received May 12, 1998

ABSTRACT: Methylglyoxal synthase provides bacteria with an alternative to triosephosphate isomerase for metabolizing dihydroxyacetone phosphate (DHAP). In the present studies, the methylglyoxal synthase gene in *Escherichia coli* has been cloned and sequenced. The identified open reading frame (ORF) codes for a polypeptide of 152 amino acids, consistent with the 17 kDa purified protein. The sequence of this protein is not similar to any other protein of known function, including the functionally similar protein triosephosphate isomerase. The methylglyoxal synthase gene was amplified by PCR, subcloned into the pET16B expression vector, and expressed in the host *E. coli* BL21(DE3). Sequence comparison of the methylglyoxal protein and related ORFs from four different bacterial species revealed that four aspartic acid and no glutamic acid residues are absolutely conserved. The function of the four aspartic acid residues was tested by mutating them to either asparagine or glutamic acid. Thermal denaturation, CD spectroscopy, and gel filtration experiments showed that the mutant enzymes had the same secondary and quaternary structure as the wild-type enzyme. Kinetic characterization of both Asp 71 and Asp 101 mutant proteins shows reduced k_{cat}/K_m by 10^3- and 10^4-fold respectively, suggesting that they are both intimately involved in catalysis. A time-dependent inhibition of both Asp 20 and Asp 91 asparagine mutants by DHAP suggests that these two residues are involved with protecting the enzyme from DHAP or reactive intermediates along the catalytic pathway. In combination with the results of 2-phosphoglycolate binding studies, a catalytic mechanism is proposed.

Methylglyoxal synthase (EC 4.2.99.11) catalyzes the conversion of dihydroxyacetone phosphate (DHAP)[1] to methylglyoxal and orthophosphate in the first step of the methylglyoxal bypass of the Embden−Myerhoff (glycolytic) pathway (*4, 5*). In *Desulfovibrio gigas*, it has been shown that this pathway and glycolysis account for 40 and 60% of polyglucose degradation, respectively (*6*). Phosphate acts as an allosteric inhibitor of the enzyme, suggesting that the methylglyoxal bypass may have significant activity under conditions of phosphate starvation. Formation of methylglyoxal is not without consequence as it is cytotoxic in millimolar quantities and has been shown to be mutagenic and to interfere with de novo protein and nucleic acid synthesis (*7*−*10*). It has been suggested that methylglyoxal excreted from bacteria may function as an antibiotic. In mammals, methylglyoxal is implicated in diabetic complications (*11*).

While methylglyoxal synthase has been purified from a variety of sources [including *Escherichia coli* (*12*), *Pseudomonas saccharophila* (*13*), *Proteus vulgaris* (*14*), *Saccharomyces cerevisiae* (*1*), and goat liver (*2*)],[2] the enzymology is best understood in *E. coli*. Purified *E. coli* methylglyoxal synthase has a reported specific activity that is nearly 2 orders of magnitude higher than that of the enzyme from other species. Further, the *E. coli* enzyme has been extensively characterized with regard to inhibitor and substrate specificity (*15*). Cells are believed to detoxify (and metabolize) methylglyoxal using glyoxalase I and glyoxalase II, which catalyze the glutathione-dependent conversion of methylglyoxal to D-lactoylglutathione and subsequently to D-lactic acid (*3*). The glyoxalase system has been detected in every species (from *E. coli* to man) in which its presence has been investigated. Interest in the glyoxalase system and methylglyoxal metabolism stems in part from its ability to clear 2-oxo aldehyde based chemotherapeutic drugs from tumors, thus rendering the treatment ineffective (*16*).

Methylglyoxal synthase catalyzes phosphate elimination utilizing a reaction mechanism similar to that of triosephosphate isomerase (Figure 1). In both mechanisms, the C-3 proton is stereospecifically abstracted to form an ene-diol(ate)−enzyme intermediate; in triosephosphate isomerase,

† This work was supported by "start-up" funds provided by the Medical College of Wisconsin (to D.H.T.H.).

* To whom correspondence should be addressed. E-mail: harrison@eeyore.biochem.mcw.edu. Phone: (414) 456-4432. Fax: (414) 456-6510.

[1] Abbreviations: CAPS, 3-[cyclohexylamino]-1-propanesulfonic acid buffer; DHAP, dihydroxyacetone phosphate; SDS, sodium dodecyl sulfate; PCR, polymerase chain reaction; P_i, inorganic phosphate; 2PG, 2-phosphoglycolate; *mgsA*, methylglyoxal synthase gene.

[2] Although there are reports of the purification of methylglyoxal synthase from *S. cerevisiae* (*1*) and goat liver (*2*) which are not widely accepted (*3*), the authors believe that these reports show little total activity and do not demonstrate proper controls for bacterial contamination.

S0006-2960(98)00409-7 CCC: $15.00
Published on Web 06/18/1998

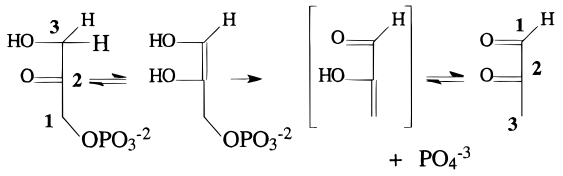

FIGURE 1: Overall reaction mechanism of methylglyoxal synthase.

this requires glutamic acid 165 (*17, 18*). Instead of protonating the C-2 position, methylglyoxal synthase directs the collapse of the ene-diol(ate) to form 2-hydroxy 2-propenal enol intermediate and orthophosphate. Since methylglyoxal synthase and triosephosphate isomerase are on parallel metabolic pathways, consume the same substrate, and utilize the same reaction intermediate, they might be related to each other by divergent evolution. Evidence supporting this hypothesis is found in a designed loop deletion mutant of triosephosphate isomerase, which confers methylglyoxal synthase-like activity upon the mutant enzyme (*19, 20*). There is also evidence to support a mechanism of convergent evolution. Unlike methylglyoxal synthase, the loop mutant of triosephosphate isomerase retains its isomerization activity and catalyzes the dephosphorylation of glyceraldehyde 3-phosphate more readily than it does DHAP (*20*). Methylglyoxal synthase abstracts the C-3 *pro*-S hydrogen of DHAP, while triosephosphate isomerase abstracts the C-3 *pro*-R hydrogen (*17*). However, unlike triosephosphate isomerase, methylglyoxal synthase is highly specific for DHAP and is not able to abstract a proton from the C-2 position of glyceraldehyde 3-phosphate. In fact, the more reactive triose phosphate isomer D-glyceraldehyde 3-phosphate acts as an inhibitor (*14*). These results indicate that the active site of methylglyoxal synthase may be quite different from that of triosephosphate isomerase.

Surprisingly, only recently has the sequence of the methylglyoxal synthase protein been reported (*21*) and described (*22*) (while this manuscript was in preparation). Here, we fully describe the independent cloning, sequencing, and overexpression of the *E. coli* methylglyoxal synthase gene. Although there is no sequence similarity between methylglyoxal synthase and triosephosphate isomerase (or any other known protein), the similarity of the mechanism requires the presence of at least one catalytic base. In triosephosphate isomerase the E165D mutant has catalytic efficiency that is 3 orders of magnitude lower than the wild-type enzyme (*23, 24*). Since there are no conserved glutamic acid residues in methylglyoxal synthase, the four conserved aspartic acid residues have been mutated to both asparagine and glutamic acid. The secondary and quaternary structure, thermal stability, and steady-state kinetics are described for each mutant enzyme. Additionally, each mutant's interaction with the transition-state analogue 2PG is described. On the basis of these findings, we propose a model of the enzyme's mechanism.

MATERIALS AND METHODS

Materials. Dihydroxyacetone phosphate dimer bis(ethyl ketal), reduced glutathione, DNase I, and yeast glyoxalase I (type III) were purchased from Sigma. Dihydroxyacetone phosphate dimer bis(ethyl ketal) was converted to DHAP by acid hydrolysis at 40 °C (*25*). PMSF was purchased from Promega Corp. T4 DNA ligase and restriction enzymes were purchased from New England Biolabs. Recombinant *pfu* DNA polymerase was purchased from Stratagene. Plasmid and genomic DNA were purified using Qiagen "midi-prep" columns and protocols. Other chemicals were purchased from Fisher Scientific. Chromatography media included Sephadex G-100 and Q Sepharose Fast Flow from Pharmacia Biotech, and Biogel P-150 from Bio-Rad. Synthetic oligonucleotides were purchased from the Protein and Nucleic Acid Shared Facility at the Medical College of Wisconsin or Life Technologies.

Purification of Native Methylglyoxal Synthase from E. coli. E. coli strain LE392 (a K-12 derivative) was grown in 12 L of Luria Broth and harvested after 5 h by centrifugation at 5000*g* for 20 min. About 36 g of cell paste was obtained and frozen at −80 °C. The cells were thawed and resuspended in 200 mL of lysis buffer (50 mM imidazole-HCl pH 7.0, 1 mM potassium phosphate, 100 μM PMSF, and 10 mg/mL DNase) and lysed using a French pressure cell at 1000 psi. The crude lysate was centrifuged at 25000*g* for 20 min at 4 °C. Methylglyoxal synthase was purified from the supernatant as described by Hopper and Cooper (*12*).

Methylglyoxal Synthase Activity Assay. The coupled assay of Hopper and Cooper (*12*) was used to determine the enzyme activity. Briefly, DHAP is converted to methylglyoxal by methylglyoxal synthase. The formation of that product is coupled to the formation of S-D-lactoylglutathione by the nonenzymatic formation to the thiohemi-acetal with glutathione and the subsequent isomerization by glyoxalase I. The rate of increase in absorbance at 240 nm, corresponding to S-D-lactoylglutathione formation, was measured on a Varian CARY 210 spectrophotometer. The standard assay mixture consisted of 0.7 mM DHAP, 15 mM glutathione, 50 mM imidazole (pH 7.0), 2 units of yeast glyoxalase I, and 10 μL of diluted methylglyoxal synthase in a total volume of 600 μL. A unit of methylglyoxal synthase activity is defined as the formation of 1 μmol of S-D-lactoylglutathione/min. A total of 1 μmol of S-D-lactoylglutathione corresponds to an absorbance of 3.4 at 240 nm. To assay for methylglyoxal synthase activity bound in a native polyacrylamide gel, the gel slices ($2 \times 6 \times 1$ mm) were minced and added to 1 mL of assay mix. After 75 min, the gel was pelleted in a microfuge and the absorbance at 240 nm was determined.

Protein Determination. Protein concentrations were determined by the Bradford dye-binding assay (*26*) (Bio-Rad) using bovine serum albumin as standard.

Electrophoresis. Native gel electrophoresis was carried out in 377 mM Tris (pH 8.8) and 10% cross-linked polyacrylamide in the presence and absence of 1 mM potassium phosphate (*27*). SDS−PAGE was carried out in 377 mM Tris (pH 8.8), 0.1% SDS, and 14% cross-linked polyacrylamide. 2-D gel electrophoresis was accomplished by running a native gel, cutting the lane out of the gel, and incubating it for 15 min in 2× SDS-sample buffer. The gel slice was then placed sideways on a SDS−polyacrylamide gel, and the proteins were further resolved by SDS−PAGE. Electrophoretic transfer of the protein to a polyvinyl difluoride membrane was carried out using a Bio-Rad "Mini-PROTEAN II" blotting chamber in 10 mM CAPS, pH 11.0, and 10% methanol at 25 V for 9 h at 4 °C. Isoelectric focusing was carried out on a Pharmacia Phast-gel system, using the Pharmacia IEF standards.

Table 1: Primers Used for Mutagenesis[a]

mutant	mutagenic primer	restriction site
A (coding, C)	5′-GGAATTCCATATGGAACTGACGACTCGCACTTT-3′	*Xho*I
B (noncoding, NC)	5′-CGGAATTCA CTCGAGTAAGAAACAGGTGGCGTTT-3′	*Nco*I
D20N (NC)	5′-AGCATTTGTTTGCAGTGATTGTGTGCCAC-3′	*Tsp*RI
D71N (C)	5′-GAGTGGCCCAATGGGGGGTAACCAGCAGGT-3′	*Hae*III
D91N (C)	5′-ATGTATTGATTTTCTTCTGGAATCCACTAAAT-3′	*Mbo*II
D101N (NC)	5′-AGACGCAGCAAGGCTTTCACGTTAGGATCGTGC-3′	*Bbv*I
D20E (NC)	5′-CCCAGCTCATCAGCATTTGTTTGCAGTGTTCGT-3′	*Alu*I
D20E (C)	5′-ACGAACACTGCAAACAAATGCTGATGAGCTGGG-3′	*Alu*I
D71E (NC)	5′-ACCTGCTGTTCACCCCCCATTGGGCCACTC-3′	*Hae*III
D71E (C)	5′-GAGTGGCCCAATGGGGGGTGAACAGCAGGT-3′	*Hae*III
D91E (NC)	5′-ATTTAGTGGTTCCCAGAAGAAAATCAATACAT-3′	*Mbo*II
D91E (C)	5′-ATGTATTGATTTTCTTCTGGGAACCACTAAAT-3′	*Mbo*II
D101E (NC)	5′-AGACGCAGCAAGGCTTTCACTTCAGGATCGTGC-3′	*Bbv*I
D101E (C)	5′-GCACGATCCTGAAGTGAAAGCCTTGCTGCGTCT-3′	*Bbv*I

[a] The mismatched base that results in the mutation of the Asp residue to Asn or Glu is in bold.

Determination of Amino Acid Sequence. A 2-μmol sample of homogeneous methylglyoxal synthase was electroblotted onto a polyvinalidene difluoride membrane and the coomassie stained band was excised for Edman degradation analysis using an Applied Biosystems model 477 Sequencer equipped with model 120A PTH-amino acid analyzer.

Polymerase Chain Reaction. The amplification protocol consisted of 5 min at 94 °C followed by 30 cycles of denaturation (94 °C, 1 min), annealing (54 °C, 1 min), and extension (72 °C, 0.5 min), followed by a cycle of extension (72 °C, 12 min). The amplification was performed in a 100 μL reaction mixture containing 1× pfu buffer (50 mM KCl, 10 mM Tris, pH 9, 0.1% Triton X-100, and 1.5 mM $MgCl_2$), 200 μM dNTP, 5 ng of genomic *E. coli* DNA or plasmid DNA, 1 μM of each primer, and 2.5 units of *pfu* DNA polymerase (Stratagene).

Sequencing the Gene. The primers 5′-CGGAATTCTAAGTGCTTACAGTAATCTGTA-3′ and 5′-CGGAATTCACTCGAGTAAGAAACAGGTGGCGTTT-3′ were used to amplify a 503 bp fragment from genomic *E. coli* (strain LE392) DNA by PCR. The genomic DNA from LE392 was purified using a Qiagen "midi-prep" column according to the manufacturer's protocol. The PCR amplified fragment was cut with the restriction enzymes *Eco*RI and *Xho*I (sites designed into the primers) and subcloned into an *Eco*RI/*Xho*I-digested pBluescript-KS(+) II vector. Both strands of three independent clones were sequenced using the Pharmacia sequencing kit and M13-universal and M13-reverse primers. The sequence was obtained using an automated DNA sequencer (ALF/Pharmacia).

Expression Vector Construction. The primers 5′-AGGATGTACACCATGGAAC TGACG-3′ and 5′-CGGAATTCACTCGAGTAAGAAACAGGTGGCGTTT-3′ were used to amplify a 456 bp fragment from genomic *E. coli* (strain LE392) DNA by PCR. The PCR amplified fragment was cut with the restriction enzymes *Nco*I and *Xho*I (sites designed into the primers) and subcloned into an *Nco*I/*Xho*I-digested pET16b vector (Novagen). The cloned coding region in the expression vector was sequenced using primers corresponding to the T7 promoter and T7 terminator region.

Construction of Asp to Asn/Glu Mutants. Each of the conserved aspartic acid residues was changed to an asparagine or glutamic acid by using PCR and mutagenic primers. Table 1 lists the sequence of the mutagenic primers for the construction of each of the following mutants: D20N/E, D71N/E, D91N/E, and D101N/E. For the asparagine mutants, a mutagenic primer and either of two primers **A** or **B** (described in Table 1) were used to form a PCR fragment that was cut with the restriction enzyme appropriate to that pair of primers. The pMGS vector containing the entire gene was similarly cut, and the wild-type sequence fragment was removed. The mutant PCR fragment was then ligated into the expression vector. For the glutamic acid mutations, site-specific mutants were incorporated into the *mgsA* gene by the method of overlap extension PCR (*28*). Here, overlapping complementary mutagenic primers are used with primers **A** and **B** to derive a mutant full-length gene. Using the restriction enzymes *Nco*I and *Xho*I, the mutant gene was subcloned into the expression vector, pET16b. Both strands of each mutant construct (the entire coding sequence) were sequenced in a Pharmacia ALF automated DNA sequencer using the Pharmacia sequencing kit and the T7-promoter and T7-terminator universal primers to verify the mutations and to ensure that no undesired mutations were present.

Bacterial Growth and Purification of Recombinant Wild-Type and Mutant Methylglyoxal Synthase. Recombinant methylglyoxal synthase was expressed in *E. coli* BL21(DE3) transformed with either a wild-type (pMGS) or mutant (pMGS-D20N, pMGS-D20E, pMGS-D71N, pMGS-D71E, pMGS-D91N, pMGS-D91E, pMGS-D101N, or pMGS-D101E) expression plasmid. An individual transformed colony was cultured at 37 °C in 1 L of LB broth supplemented with ampicillin (100 μg/mL) until the media reached an optical density of about 0.8 at 600 nm. IPTG was added to a final concentration of 1 mM, and the incubation was continued for 4 h. Cells were harvested by centrifugation at 5000*g* for 20 min, and the pellets were stored at −80 °C prior to cell lysis. The bacterial pellet was resuspended in 40 mL of 50 mM imidazole, pH 7.0, and 1 mM potassium phosphate (buffer A) at 4 °C and lysed using a French pressure cell operating at 1000 psi. The crude lysate was centrifuged at 25000*g* for 25 min at 4 °C. The supernatant was heated rapidly in a boiling water bath, with continuous stirring to 70 °C, kept at this temperature for 1 min, and then quickly cooled to 0 °C in an ice−water bath. The heavy precipitate was removed by centrifugation at 25000*g* for 25 min at 4 °C. The supernatant was applied to a FastQ anion-exchange column (8 × 1.5 cm) equilibrated with buffer A, and the column was then washed with 60 mL of the

equilibrating buffer. The protein was eluted from the column using a gradient of 0−500 mM NaCl in buffer A at 1 mL/min; 2.0 mL fractions were collected. The fractions were analyzed spectrophotometrically for activity and by SDS−PAGE for purity.

Analytical Gel Filtration Chromatography. A Superose-12/30 gel filtration chromatography column was equilibrated in a 50 mM imidazole buffer, pH 7.0, containing 1 mM potassium phosphate and 350 mM NaCl. The column was calibrated with 100 μg of cytochrome *c* (12 400), trypsinogen (23 500), ovalbumin (45 000), bovine serum albumin (66 200), and HMG-CoA reductase (114 000). A standard curve was fit to the log of the molecular weight versus $(v_e - v_o)/(v_t - v_o)$.

Enzyme Kinetics. Kinetic constants for the wild-type and mutant enzymes were determined in the same manner as was used to determine the enzyme activity except that the concentration of DHAP was varied. For simple kinetics, each data point (initial velocity) was determined in triplicate and at least five different substrate concentrations were examined. For kinetics involving the competitive inhibitor 2PG, each data point (initial velocity) is uniquely represented on the corresponding graph (shown in conjunction with tabulated kinetic parameters). Control assays, lacking either substrate or enzyme, were routinely included and found to be negligible over the time course of the assay. Kinetic constants were calculated by fitting the Michaelis−Menten function directly in hyperbolic form to the data with an unweighted least-squares analysis using the program GRAFIT (*29*). Steady-state kinetics in the presence or absence of inhibitors were analyzed by one of the following equations:

$$v_i = VA/(K_m + A) \quad (1)$$

$$v_i = VA^h/(K_m + A^h) \quad (2)$$

$$v_i = VA/[K_m(1+ I/K_i) + A] \quad (3)$$

$$v_i/V = \alpha(1 + \alpha + \theta)^{n-1}/[L + (1 + \alpha + \theta)^n],$$
$$\alpha = [E_R(\mathrm{DHAP})]/[E_R] = [\mathrm{DHAP}]/K_{d,\mathrm{DHAP}}, \text{ and}$$
$$\theta = [E_R(2\mathrm{PG})]/[E_R] = [2\mathrm{PG}]/K_{d,2\mathrm{PG}} \quad (4)$$

Where v_i is the observed velocity, V is the maximal velocity, A is the substrate concentration, I is the inhibitor concentration, h is the Hill coefficient, K_m is the Michaelis−Menten constant, and K_i is the competitive inhibition constant. Equation 2 was used for analyzing kinetics in the presence of phosphate. If the value of the Hill coefficient was less than 1.1, then eq 1 was used. Equation 3 was used for 2-phosphoglycolate (2PG) inhibition studies. For fitting 2PG inhibition data in the presence of phosphate, eq 4 was used, where the parameters α and θ are functions of the substrate or competitive inhibitor binding to the enzyme in the relaxed state. These parameters may be thought of either as the ratio of bound relaxed enzyme to free relaxed enzyme or empirically as the ratio of the small molecule (substrate or competitive inhibitor) concentration to the equilibrium constant for the relaxed enzyme (*30*). The parameter L is the ratio of the concentration enzyme in the taut state to that in the relaxed state at a given phosphate concentration ($L = [E_T]/[E_R]$) in the absence of substrate or competitive inhibitor, and the parameter n is the number of active sites that can interact.

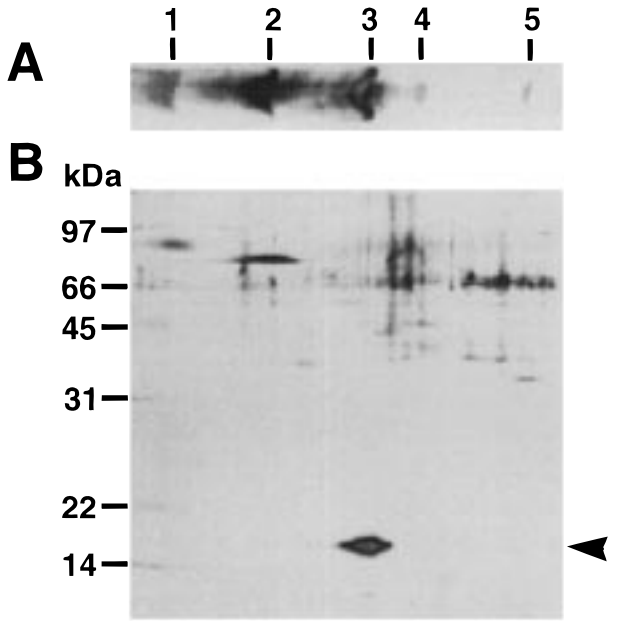

FIGURE 2: Silver-stained gel of partially purified methylglyoxal synthase. (A) Slice of native gel used to identify the band containing methylglyoxal synthase activity. (B) The bands from the native gel slice were resolved by running a second denaturing dimension, the band pointed to corresponds to a molecular mass of 17 kDa.

CD Spectroscopy and Melting Temperature Determination. A solution containing 1 μM of wild-type or mutant protein was prepared in 15 mM Tris-acetate, pH 7.0, in the presence or absence of 1 mM potassium phosphate. A cuvette (0.1 cm) containing this solution was placed in a Jasco 710 CD spectrometer, and a near-UV CD spectrum was obtained from 190 to 260 nm. A "melting temperature" for the wild-type and each mutant was obtained by monitoring the CD ellipticity at 208 nm while raising the temperature from 30 to 90 °C at a rate of 1 °C/min.

RESULTS

Purification of the Endogenous E. coli Protein and Its Quaternary Structure. Following the procedure of Hopper and Cooper (*12*), methylglyoxal synthase was purified 560-fold from an *E. coli* extract. Native gel analysis confirmed the previous results: five distinct bands could be detected, three of which are dominant (*12*). As previously reported, the mobility of the third band shifted when phosphate was present in the gel running buffer. To determine which band(s) contained methylglyoxal synthase activity, equal amounts of protein were run on two lanes of a native gel. One lane was visualized by silver staining (Figure 2a). Equivalently sized sections corresponding to the five stained bands and one section which showed no protein band were cut from the unstained gel. Each gel slice was assayed for methylglyoxal synthase activity. After subtracting the background activity of the gel slice without protein, only the third band on the gel showed significant methylglyoxal synthase activity (Table 2). Although the apparent molecular mass of methylglyoxal synthase had been reported to be about 67 kDa by gel filtration, the protein was not previously characterized by SDS−PAGE (*12*). Two-dimensional gel

Table 2: Assay of Methylglyoxal Synthase Activity Found in Each Band Detected in the Native Gel

slice	product formed[b]	excess product[c]
1	106	35
2	71	0
3	403	332
4	50	−21
5	38	−33
NP[a]	71	

[a] No protein in gel slice. [b] Nanomoles of methylglyoxal produced. [c] Nanomoles of methylglyoxal produced after subtracting the methylglyoxal formed from a gel slice lacking protein.

Table 3: Comparison of the Amino Acid Analysis of Methylglyoxal Synthase to the Amino Acid Composition Predicted by the Cloned Gene

	methylglyoxal synthase protein—experimental		methylglyoxal synthase gene	
residue name	amino acid mole percent	est. no. of residues	calculated mole percent	no. of residues
Asp and Asn	10.077	15	11.842	18
Thr	5.146	8	6.579	10
Ser	2.151	3	3.289	5
Glu and Gln	20.135	30	7.237	11
Pro	6.264	9	5.921	9
Gly	6.104	9	5.263	8
Ala	9.395	14	9.868	15
Val	7.978	12	7.895	12
Met	3.163	5	3.947	6
Ile	5.604	8	6.579	10
Leu	10.917	16	11.842	18
Tyr	1.809	3	1.974	3
Phe	2.615	3	2.632	4
His	2.973	4	4.605	7
Lys	2.257	3	3.289	5
Arg	3.412	5	4.605	7
Trp	NA	NA	1.974	3
Cys	NA	NA	0.658	1

analysis (native in the first dimension and SDS-denaturing in the second dimension) revealed that the molecular mass of the band corresponding to gel slice 3 on the native gel is 17 kDa (Figure 2b).

Peptide Sequence Analysis. Methylglyoxal synthase purified by two-dimensional gel electrophoresis was electroblotted onto a PVDF membrane for total amino acid analysis and amino-terminal sequence analysis. The results of the amino acid analysis (Table 3) were used to search a protein sequence database using the "EMBL-Heidelberg Amino Acid Analysis Server" (*31*). This search identified a "hypothetical protein" from *Haemophilus influenza* with a reliability score between 82 and 88%. The reliability score of the next most significant match was between 68 and 75%. The results of the amino-terminal sequencing (Figure 3) were used to search the nonredundant translated DNA database using FASTA (*32*). This search identified an *E. coli* open reading frame (ORF, SwissProt:YCCG_ECOLI) found at the 3′-end of *helD* gene [genebank: J04726 (*33*)] which is identical to 22 of the 23 amino acid determined by amino-terminal sequencing. However, the ORF obtained from the database showed an additional 17 amino acids upstream of the start of the determined protein sequence. Additionally, the *E. coli* ORF shows 59% identity to the hypothetical protein from *H. influenza* identified in the amino acid composition search.

Cloning of DNA Encoding Methylglyoxal Synthase. The *E. coli* ORF YCCG_ECOLI including the 5′-flanking sequence was amplified by high-fidelity PCR from genomic *E. coli* DNA using primers with convenient restriction sites at their 5′-ends. The amplified DNA was cloned into pBluescript II KS+ (Stratagene) and sequenced. The sequencing of three independent clones revealed an error in the database corresponding to an additional adenosine (number 54 in our sequence). Subsequently, the *E. coli* genome project and others have sequenced this region confirming our sequence (*22, 34*). This new DNA sequence predicts an ORF that starts at one of two possible methionines (Figure 3).

Comparison to Other DNA Sequences. The program TBLASTN (*35*) was used to search the nonredundant translated DNA database with the *E. coli* protein sequence. The search found the following similar ORFs or hypothetical proteins from five species including the *H. influenza* sequence detected earlier by amino acid composition: *E. coli* (sp, P37066), *H. influenza* (sp, L45868), *Bacillus abortus* (gp, U21919), *Bacillus subtilus* (gb, L38424), and *Synechocystis* (gb, D64006) (Figure 4). Surprisingly, no known protein sequence was found to be similar to the *E. coli* sequence.

Expression and Purification of Wild-Type and Mutant Methylglyoxal Synthase. The identity of the methylglyoxal synthase gene (*mgsA*) was verified by the overexpression and subsequent purification of the gene product. The DNA fragment coding for a 152 amino acid protein was amplified by high-fidelity PCR from genomic *E. coli* DNA and cloned into pET16b (Novagen). The 5′-primer was designed so that the ATG corresponding to the second methionine replaced the ATG of the expression vector. The coding region of the pMGS vector was sequenced to ensure the fidelity of the PCR reaction. Transformed BL21(DE3) cells containing the pMGS vector were induced with IPTG. Approximately 30% of the soluble protein was found to have a molecular mass of 17 kDa by SDS−PAGE. There was a 5000-fold increase in the methylglyoxal synthase activity in the crude lysate of cells containing the pMGS vector compared to cells containing the pET16b vector alone. pET16b vectors containing the gene for the mutant enzyme were constructed and expressed in a similar manner (Materials and Methods).

The purified methylglyoxal synthase was shown to be greater than 99% pure on either a coomassie stained SDS−polyacrylamide gel or isoelectric focusing gel. On a calibrated gel filtration column, the recombinant enzyme was found to have an apparent molecular mass of 67 kDa as reported by Hopper and Cooper (*36*) for the endogenous protein. Like the endogenous protein, the recombinant protein ran with greater mobility on a native gel in the presence of phosphate than it did in the absence of phosphate. The expression and purification of the mutant methylglyoxal synthase proteins was remarkably similar to that of the wild-type enzyme. One exception was that 95% of the D91E mutant protein precipitated upon heat treatment; the remaining 5% was nonetheless purified by anion-exchange chromatography. For the other enzymes, the specific activity remained the same after the heat-denaturing step, although qualitatively, the proteins on an SDS gel appeared cleaner. Unlike the purification of the endogenous enzyme, a 50% loss of total activity was observed for each of the other recombinant enzymes. This step was retained as being critical in the purification of the endogenous enzyme and

```
                          1                                    **                  *    60

genebank:J04726           TAAGTGCTTACAGTAATCTGTAGGAAAGTTAACTCAGGATGTACATTATGGAAACTGACG

new sequence              TAAGTGCTTACAGTAATCTGTAGGAAAGTTAACTACGGATGTACATTATGGAA CTGACG

N-terminal protein sequence                                                ?  E   L  T

SwissProt:YCCG_ECOLI *  V  L  T  V  I  C  R  K  V  N  S  G  C  T  L  W  K  L  T

translation                                                                M  E   L  T

alternative translation                                        M  Y  I  M  E   ...


                          61                                                        120

genebank:J04726           ACTCGCACTTTACCTGCGCGGAAACATATTGCGCTGGTGGCACACGATCACTGCAAACAA

New sequence              ACTCGCACTTTACCTGCGCGGAAACATATTGCGCTGGTGGCACACGATCACTGCAAACAA

N-term prot. seq.         T  R  T  L  P  A  R  K  H  I  A  L  V  A  H  D  H  C  K  Q

SwissProt:YCCG_ECOLI T  R  T  L  P  A  R  K  H  I  A  L  V  A  H  D  H  C  K  Q

New translation           T  R  T  L  P  A  R  K  H  I  A  L  V  A  H  D  H  C  K  Q
```

FIGURE 3: The DNA sequence found in the database and a comparison between the translated protein sequence and the sequence determined by Edmund degradation analysis. The identity of the first residue was not discernible. The incorrect bases in the database sequence are highlighted. The ribosome-binding site is underlined. The expected translation based on its position relative to the ribosome--binding site and the observed amino-terminal sequence is shown. An alternative in-frame start site is also shown.

may have been removed from the purification of the recombinant enzymes. The aspartic acid to asparagine mutants eluted from the anion exchange-column about two fractions (2 mL fractions of a 150 mL gradient as described) earlier than the wild-type enzyme. However, all of the mutant proteins had the same mobility on either a calibrated gel filtration column or a SDS−polyacrylamide gel.

CD Spectroscopy and Thermal Stability. CD spectra of the wild-type and all mutant enzymes were taken in both the presence and the absence of 1 mM potassium phosphate. All of the spectra were essentially identical within the error of the measurement. The spectra were consistent with a protein that had both α-helices and β-sheets (no attempt has been made to quantify these data). The thermal stability of each of the proteins was measured by monitoring the ellipticity at 208 nm as the temperature of the cuvette was raised from 25 to 90 °C at a rate of 1 °C/min. The magnitude of the ellipticity at 208 nm dropped dramatically as the protein went through the transition, and the "melting" temperature was recorded (Table 4). The addition of phosphate stabilized all of the mutants, but not as much as it stabilized the wild-type enzyme.

Kinetic Studies of Wild-Type Recombinant Methylglyoxal Synthase. The purified recombinant protein had a specific activity of 1133 units/mg. Fitting velocity data to the Michaelis−Menten equation, the apparent K_m for DHAP is 0.20 ± 0.03 mM and the k_{cat} value is 220 s^{-1}, giving a k_{cat}/K_m of 1.1×10^6 M^{-1} s^{-1} for the recombinant enzyme. The value for K_m is in good agreement with the value of 0.47 mM previously reported for the native enzyme (*12*). In the presence of 0.2 or 0.3 mM phosphate, the enzyme kinetics become sigmoidal (Figure 5a). Fitting the data to eq 2 gave Hill coefficients of 2.2 and 3.4, respectively, which is in good agreement with the previously determined value of 2.6 (*12*).

Effect of Mutations on Enzyme Kinetics. All of the mutations to the four aspartic acids had an effect on k_{cat} and little effect on K_m (Table 5). In general, mutating an aspartic acid residue to a glutamic acid results in a less severe change to the kinetics than does the mutation to an asparagine. Under the conditions of the assay, activity of neither the mutant D20N nor the mutant D91N could be measured due to time-dependent substrate inhibition of these enzymes. By time-dependent substrate inhibition, it is meant that, at low enzyme concentrations, the activity of each of these two mutant enzymes decays exponentially in the presence of DHAP. The rate of decay of mutant enzyme activity is too large to reliably estimate an initial rate. Further, it is not possible to quantitate the rate of this time-dependent substrate inhibition without stopped-flow instrumentation.

The Effect of Mutations on Enzyme Kinetics in the Presence of 0.3 mM Phosphate. Again, the kinetics for the D20N mutant were unmeasurable due to time-dependent substrate inhibition. Interestingly, in 4 mM phosphate, the D20N mutant is no longer subject to time-dependent substrate inhibition and is, in fact, a better enzyme (faster rate of turnover) than wild-type at physiological levels of DHAP. In the presence of 0.3 mM phosphate, changes in the apparent K_m were significant for the D20 and D101 mutants. The Hill coefficient was dramatically reduced for all of the mutants studied (Table 6).

2-Phosphoglycolate as an Inhibitor of Methylglyoxal Synthase. The structure of 2PG is analogous to the structure of the ene−diolate intermediate (Figure 5b). This molecule has been used as a competitive inhibitor in studies of triosephosphate isomerase (*37*, *38*). As expected from the proposed mechanism, 2PG is a competitive inhibitor of methylglyoxal synthase with an inhibition constant of 2.0 μM (Table 7). This inhibitor was used to show that

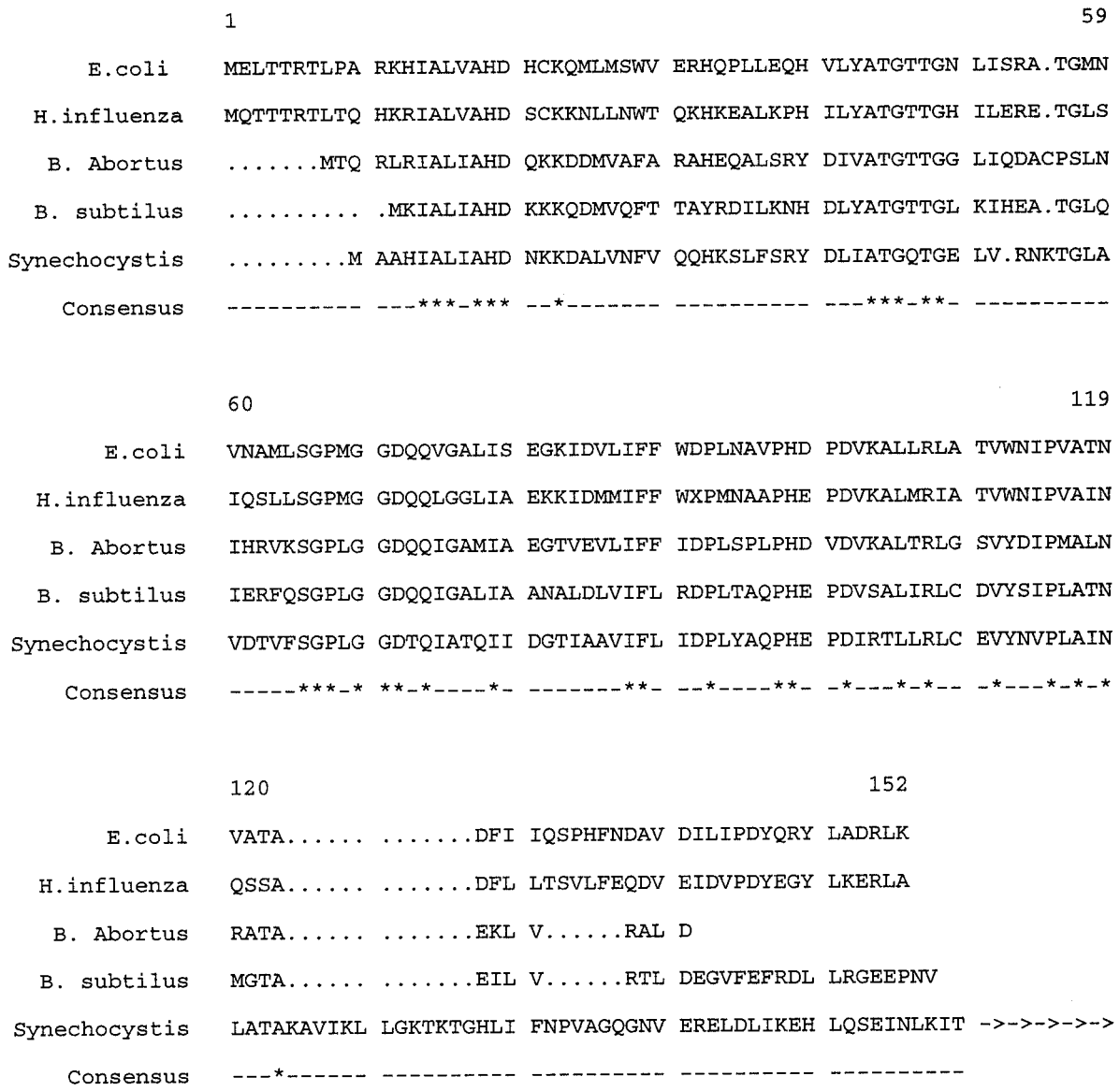

FIGURE 4: An alignment of the protein sequence of *E. coli* methylglyoxal synthase with the ORFs identified in other species.

Table 4: Melting Temperatures for Wild-Type and Mutant Methylglyoxal Synthase

	0 mM P_i		+1 mM P_i		
protein	T_m (°C)	ΔT_m (wt)	T_m (°C)	ΔT_m (wt)	ΔT_m (P_i)
wt	65.3		70.8		5.5
D20E	67.0	1.7	69.5	−1.3	2.5
D20N	59.9	−5.4	62.4	−8.4	2.5
D71E	67.5	2.2	69.2	−1.6	1.7
D71N	63.6	−1.7	66.5	−4.3	2.9
D91N	61.5	−3.8	64.9	−5.9	3.4
D101E	62.8	−2.5	67.7	−3.1	4.9
D101N	59.9	−5.4	63.9	−6.9	4.0

phosphate is a true allosteric inhibitor. The initial velocity for the wild-type enzyme was measured in the presence of 0.41 mM DHAP and 0.3 mM phosphate while the amount of 2PG was varied (Figure 6a). The plot of $1/v$ vs 2PG concentration shows an initial increase in activity on the addition of up to 4 μM 2PG. These data were fit to eq 4 (Table 7). Both k_{cat} and K_m are in good agreement with the values determined in the absence of any inhibitors. Interestingly, the number of interacting active sites is found to be 3.8 ± 0.9. The significance of these results is discussed below.

Effects of 2-Phosphoglycolate on the D71 and D101 Mutants. 2PG is a competitive inhibitor of the D71N mutant enzyme as shown by the double reciprocal plot (Figure 6b). The data were fit to eq 3, which shows that the K_i for 2PG is 4.1 μM (Table 7). The plot of the apparent K_m/V_{max} versus the inhibitor concentration shows a nearly linear relationship. However, the plot of the apparent K_m/V_{max} versus the inhibitor concentration shows an initial increase in activity for the D71E mutant (Figure 6c). This increase in activity is reminiscent of the wild-type enzyme in the presence of 0.3 mM phosphate (Figure 6a). The activity increases (the apparent K_m/V_{max} decreases) going from 0 to 10 μM 2PG. The initial velocity for the D71E mutant enzyme was measured in the presence of 0.41 mM DHAP while the amount of 2PG was varied (Figure 6d). The fit of these data to eq 4 gave values of k_{cat} of 0.83 s^{-1}, K_d of 0.7 mM, and K_i of 3.7 μM (Table 7). More remarkably, the plot of the apparent K_m/V_{max} versus the inhibitor concentration for the mutant D101E shows that it is activated by 2PG up to concentrations of 0.5 mM (Figure 6e). The initial velocity

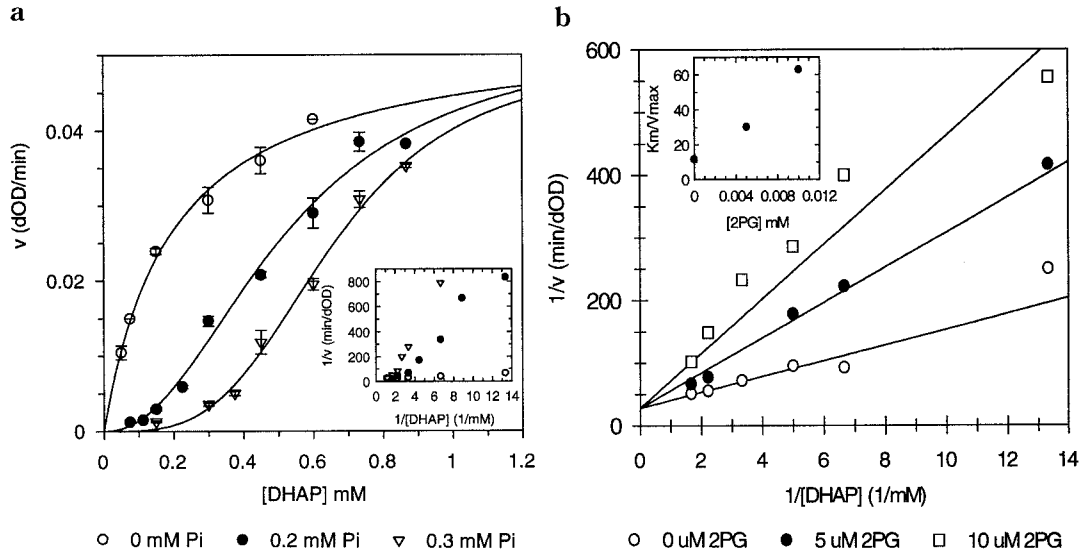

FIGURE 5: (a) Initial velocity plotted versus substrate concentration in the absence of phosphate (open circles), with 0.2 mM phosphate (filled circles) and with 0.3 mM phosphate (open inverted triangles). The inset shows the double reciprocal plot for the same data, note that the phosphate inhibited plots may be fit by power function. (b) A double reciprocal plot showing competitive inhibition by 2PG for the wild-type enzyme in the absence of phosphate. Inset shows the replot of K_m/V_{max} versus 2PG concentration confirming the competitive nature of the inhibition.

Table 5: Kinetic Constants for wt and Mutant MGS at 0.0 mM P_i

	K_M (mM)	k_{cat} (s^{-1})	k_{cat}/K_M ($mM^{-1}\,s^{-1}$)	fold inactivation
wt	0.20 ± 0.03	220 ± 10	1100	
D20N	ND	ND	ND	ND
D20E	0.18 ± 0.07	0.959 ± 0.144	5.3	2.1×10^2
D71N	0.12 ± 0.02	0.0918 ± 0.0048	0.77	1.4×10^3
D71E	0.38 ± 0.04	0.248 ± 0.013	0.65	1.7×10^3
D91N	ND	ND	ND	ND
D91E	0.41 ± 0.03	0.564 ± 0.019	1.4	7.9×10^2
D101N	0.65 ± 0.07	0.0476 ± 0.0024	0.073	1.5×10^4
D101E	0.33 ± 0.04	0.0648 ± 0.0033	0.20	5.5×10^3

Table 6: Apparent Kinetic Constants for wt and Mutant Methylglyoxal Synthase in the Presence of P_i

	0.3 mM P_i		Hill coefficient	equation used
	K_M (mM)	k_{cat} (s^{-1})		
wt	0.23 ± 0.16	203 ± 39	3.47 ± 0.61	2
D20N	ND	ND		
D20E	1.25 ± 0.10	0.830 ± 0.029	1.32 ± 0.04	2
D71N	0.13 ± 0.01	0.0706 ± 0.0034		1
D71E	0.73 ± 0.07	0.225 ± 0.010		1
D91N	0.56 ± 0.07	1.60 ± 0.092		1
D91E	0.067 ± 0.021	0.148 ± 0.005	1.4 ± 0.1	2
D101N	0.98 ± 0.07	0.0227 ± 0.0007		1
D101E	2.81 ± 0.33	0.0514 ± 0.0029		1

for the D101E mutant enzyme was measured in the presence of 0.41 mM DHAP, while the amount of 2PG was varied (Figure 6f). The fit of these data to eq 4 gave values of k_{cat} of 5.4 s^{-1}, K_d of 1.95 mM, and K_i of 760 μM (Table 7). However, the most peculiar kinetic behavior is that of the D101N mutant, where 2PG is an uncompetitive inhibitor with a K_{ii} of 66 μM (Figure 6g).

DISCUSSION

The hydrodynamic behavior of native protein on a gel filtration column (68 kDa) suggests that methylglyoxal synthase forms a homotetramer in solution. This stoichiometry is consistent with the finding that the inhibition of the enzyme by phosphate is allosteric with an estimated Hill coefficient that is between 2.2 and 3.4. However, the molecular mass determined by gel filtration is subject to a number of assumptions including that the assembly does not interact with the gel matrix and that the assembly is essentially spherical. To further probe the oligomeric state of the enzyme, the competitive inhibitor 2PG was used in combination with phosphate to determine the number of interacting active sites. In this experiment, it is expected that the observed rate of catalysis for a fixed quantity of substrate in the presence of an allosteric inhibitor will increase in the presence of a small quantity of a competitive inhibitor. This is exactly what is observed for the wild-type enzyme (Figure 6a). The competitive inhibitor binds to one of the monomers (forcing it to the "relaxed" conformation). The intersubunit forces that confer cooperativity will shift the equilibrium of the other monomers from the "taut" (inactive) to the "relaxed" (active) state, thus activation (*30*). In other words, the competitive inhibitor will act as an activator by shifting the equilibrium from the "taut" toward "relaxed" state of the enzyme complex. The parameters α and θ used in eq 4 give rise to K_d for DHAP and a K_i for 2PG which are comparable to the K_m and K_i derived independently (Figure 5b and Table 7). Although the kinetic parameters K_i, K_d, and k_{cat} are not in perfect agreement with independent measurements, the number of interacting active sites in a molecule of methylglyoxal synthase was found to be 3.8 (Table 7). These data are consistent with a molecular assembly that is at least a homotetramer in size.

The amino acid composition combined with the molecular weight and the amino-terminal peptide sequence of endogenous methylglyoxal synthase allowed us to identify and sequence its gene (*mgsA*). The gene sequence revealed two potential methionine start sites for the protein. Both the position of the ribosome-binding site and the amino-terminal peptide sequencing results suggested that the second (in frame) AUG is the authentic start site. The second start site has a ribosome-binding site (ACGGA) that is the optimal

Table 7: Response of Wild-Type and Mutant Methylglyoxal Synthase to the Competitive Inhibitor 2-Phosphoglycolate

	[DHAP] (mM)	[P_i] (mM)	k_{cat} (s^{-1})	K_d (DHAP) (mM)	L	n	K_i (2PG) (μM)	equation
WT	0.075−0.6	0.0	324 ± 31	0.16 ± 0.04[a]	NA	NA	2.0 ± 0.4	3
D71N	0.075−0.6	0.0	0.083 ± 0.003	0.08 ± 0.01[a]	NA	NA	4.1 ± 0.7	3
D101N	0.015−1.0	0.0	0.047 ± 0.002	0.64 ± 0.05[a]	NA	NA	66 ± 7[b]	3
WT	0.41	0.3	600 ± 98	0.53 ± 0.12	15.7 ± 6.4	3.8 ± 0.9	5.6 ± 1.4	4
D71E	0.41	0.0	0.83 ± 2.0	0.7 ± 2.7	9.4 ± 49	4.0 ± 0.7	3.7 ± 4.9	4
D101E	0.41	0.0	5.4 ± 10.8	1.95 ± 5.3	150 ± 623	9.5 ± 1.5	760 ± 350	4

[a] This is K_m, not K_d. [b] Uncompetitive inhibition constant K_{ii}.

distance, −8 nucleotides from the AUG initiation codon, for initiating translation. In the analysis of the upstream DNA sequence, a second ribosome-binding site (TAGGA) is observed −14 nucleotides from the first AUG start site. Although the sequence of this ribosome-binding site is closer to the consensus ribosome-binding site, the distance of 14 nucleotides makes it unlikely to initiate translation. The first (in frame) AUG may turn out to be a "cryptic" start site. However, there is no amino acid sequencing evidence to support this possibility and further study would be required to evaluate the potency of this start site. The expressed recombinant protein appears to have the same activity, gel filtration mobility, and allosteric properties as the endogenous protein.

In addition to the bacterial organisms in which methylglyoxal synthase has been detected (*12*) [i.e. *E. coli*, *P. saccharophila* (*13*), *Aerobacter aerogenes* (*12*), *Serratia marcescens* (*12*), *P. vulgaris* (*14*), *D. gigas* (*6*), and *Erwinia uredovora* (*12*)], four additional organisms that have a gene with a high degree of similarity to the *E. coli* gene are reported here: *H. influenza*, *B. abortus*, *B. subtilus*, and *Synechocystis*. Interestingly, Hopper and Cooper (*36*) found no enzyme activity in *B. subtilus* crude lysates. It is also interesting that the carboxy-terminus of the *Synechocystis* protein is distantly related to a *B. subtilus* protein (bmrU) which coexpresses with the multidrug resistance regulatory protein. The fact that no similarity was found between the *E. coli* gene and any eukaryotic sequence does not contradict the widely held belief that methylglyoxal synthase is strictly a bacterial enzyme.

Methylglyoxal synthase and triosephosphate isomerase share a number of common features. Both enzymes initiate the reaction by the abstraction of a proton from the C-3 carbon of DHAP to form an ene-diol(ate). The apparent K_m for DHAP (about 0.5 mM) is nearly the same for both enzymes. The fact that the sequence of methylglyoxal synthase is unrelated to triosephosphate isomerase [compared using the program GAP (*39*)] suggests that a mechanism of convergent rather than divergent evolution played a role in overcoming some of the same binding and catalytic challenges presented by both mechanisms. Since the uncatalyzed rate of elimination is 100-fold larger than the rate of isomerization for DHAP, the evolutionary pressure on the product specificity exhibited by methylglyoxal synthase would be less than that on triosephosphate isomerase. Where triosephosphate isomerase must have evolved a flexible loop to set the C3−C2−C1−O(P) dihedral angle of DHAP to reduce the probability of phosphate elimination (*20*), ancestral methylglyoxal synthases needed only to form an ene-diolate to be an effective catalyst.

The amino acid sequence of methylglyoxal synthase reveals a number of interesting features. The high number of conserved and nonconserved proline residues (approximately 6%) may help to explain the observed thermal stability of the protein. Analysis of the sequences revealed three distinct regions as being conserved, 13-IALvAHDxxK, 42-LyATGtTG, and 66-SGPmGGDqQ (Figure 3). Interestingly, both the second and third identified regions each have two glycines, suggesting that they may be loop regions. Since no glutamic acid residue is conserved, it is likely that one of the four conserved aspartic acid residues will act as the catalytic base to abstract the C-3 proton. To verify this hypothesis, each aspartic acid has been changed to either an asparagine (which is isosteric, but lacks a negative charge) or a glutamic acid (which conserves the negative charge, but displaces it by one methylene group). The CD spectra and gel filtration mobility of each mutant confirm that both the secondary and quaternary structure remain largely unchanged. The thermal stability of the mutant proteins would also appear to be similar to the wild-type protein, as "melting temperatures" are within 5 °C of that of the wild-type enzyme with the exception of D20N and D101N (Table 4). As the kinetic data were taken at a temperature well below the melting temperature of the most affected mutant protein, protein stability must not be contributing to the kinetic results.

Kinetic analysis of the mutant enzymes yields the somewhat unexpected result that each conserved aspartic acid residue is important to the overall catalytic efficiency of this enzyme. In the absence of phosphate, both the D20N and the D91N mutants were intolerant of the presence of DHAP and displayed time-dependent substrate inhibition. The activity of both of these mutant enzymes would decrease to zero activity in a DHAP-dependent manner over the course of five or fewer minutes. Both of these enzymes were insensitive to the addition of the reaction product (methylglyoxal) to the assay mix. Further, both of these enzymes would remain active in the presence of large quantities of phosphate (>1 mM). The corresponding mutants D20E and D91E did not exhibit such behavior. We suggest that a negative charge is necessary near these two locations (both of which may be near the allosteric phosphate binding site) to protect the enzyme from reacting with either DHAP or an intermediate along the reaction pathway. It is possible that the role for these two aspartic acid residues is to keep a lysine residue in the active site (perhaps Lys 23, Figure 4) from forming a Shiff-base with the keto oxygen of DHAP. If the reaction proceeded, the ultimate product would be the secondary amine of the anticipated ene-ol aldehyde product (Figure 7a). Such a complex would be slow to hydrolyze and render the enzyme inactive. However, we currently have no evidence of a covalently modified enzyme. On the basis of the relatively high activities for the D20 and D91 mutants in the presence of phosphate and the observed time-

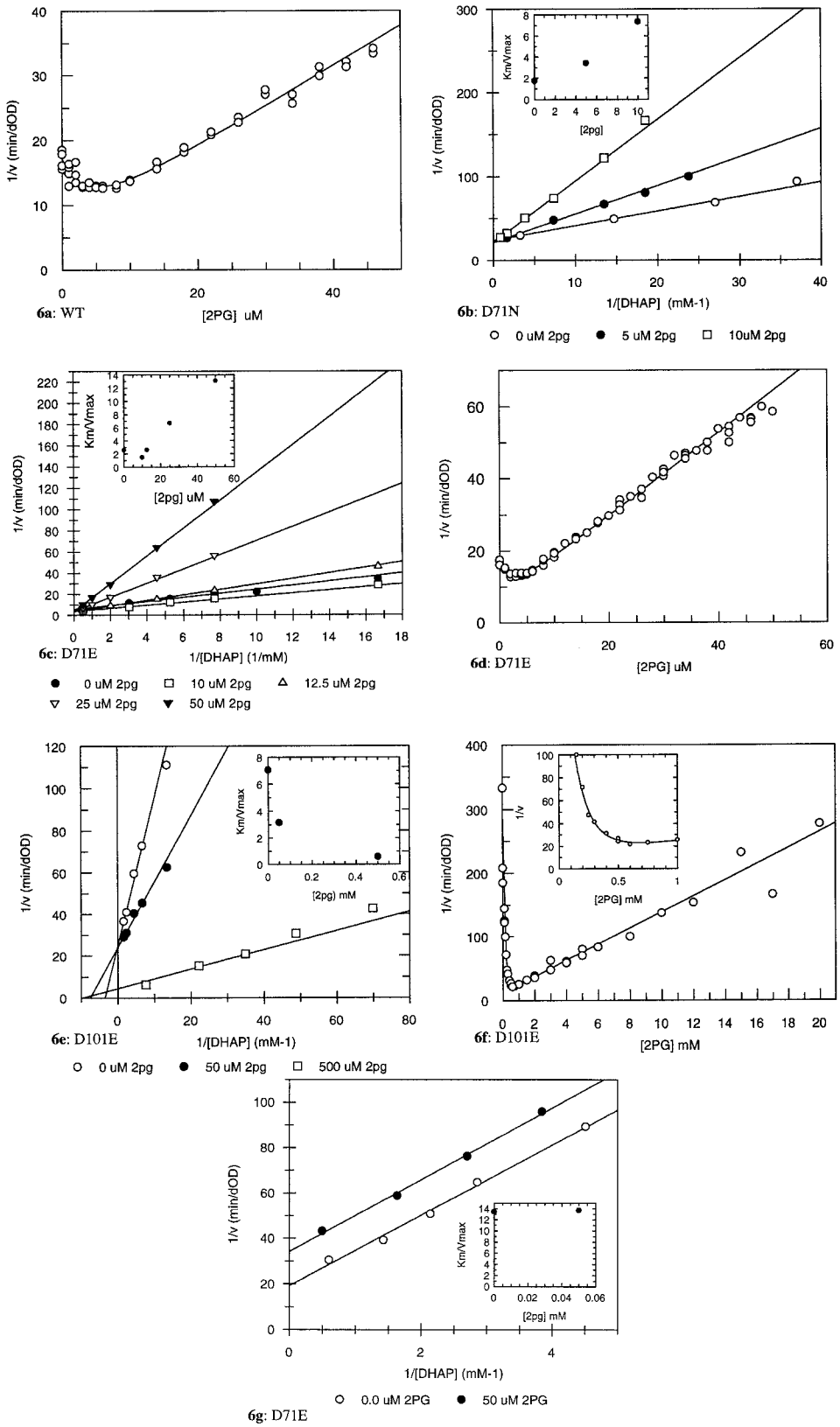

FIGURE 6: (a) The effect of 2PG on the velocity of wild-type methylglyoxal synthase with a fixed amount of DHAP (0.41 mM) in the presence of 0.3 mM phosphate. (b) A double reciprocal plot showing competitive inhibition by 2PG for the D71N mutant in the absence of phosphate. Inset shows the replot of K_m/V_{max} versus 2PG concentration confirming the competitive nature of the inhibition. (c) A double reciprocal plot showing activation followed by inhibition for 2PG with the D71E mutant in the absence of phosphate. Inset shows the replot of K_m/V_{max} versus 2PG concentration showing a pattern similar to that of panel a. (d) The effect of 2PG on the velocity of D71E mutant with a fixed amount of DHAP (0.41 mM). (e) A double reciprocal plot showing activation by 2PG for the D101E mutant in the absence of phosphate. Inset shows the replot of K_m/V_{max} versus 2PG concentration showing a pattern similar to the initial portion of panel a. (f) A Dixon plot showing the effect of 2PG on the velocity of D101E mutant with a fixed amount of DHAP (0.41 mM). The inset graph shows the fit in a region of the curve corresponding to the other figures. (g) A double reciprocal plot showing uncompetitive inhibition by 2PG for the D101N mutant in the absence of phosphate. Inset shows the replot of K_m/V_{max} versus 2PG concentration confirming the uncompetitive nature of the inhibition.

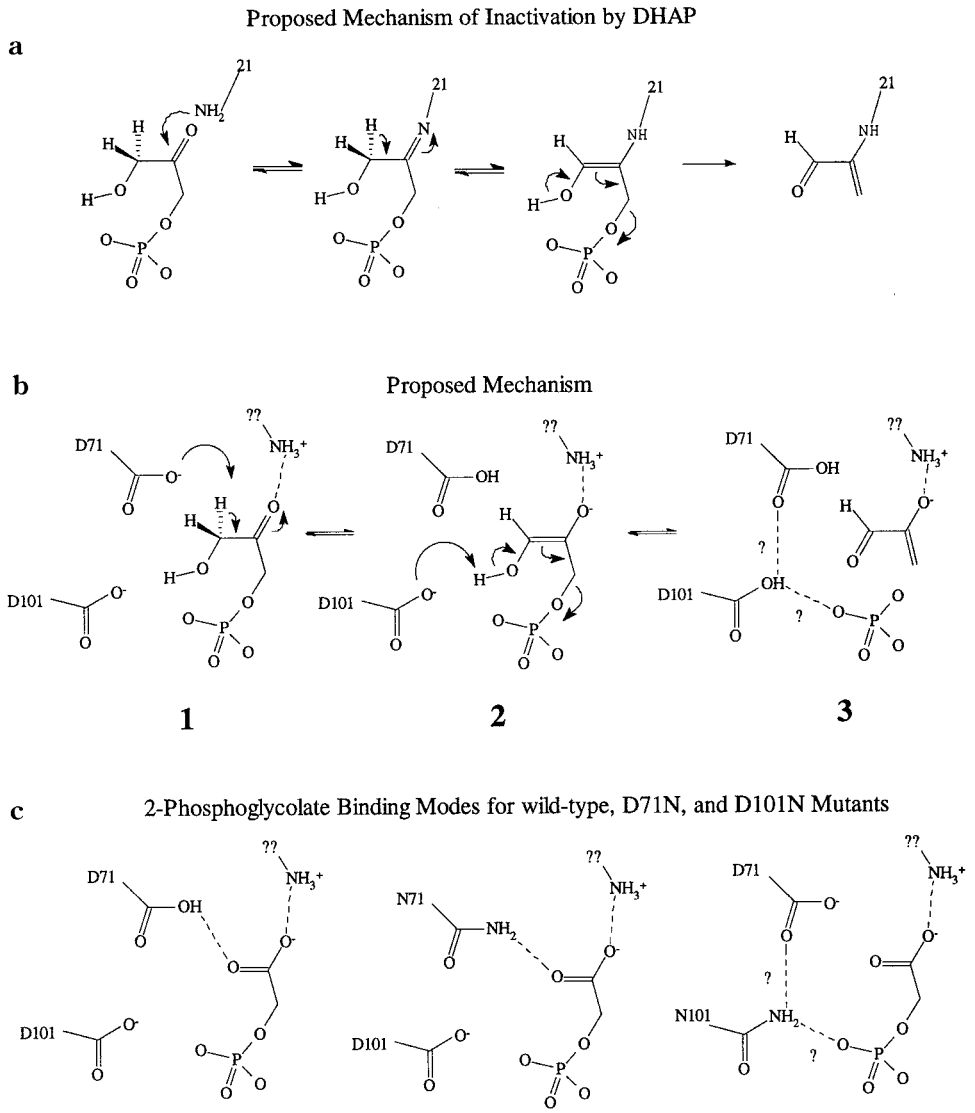

FIGURE 7: (a) A mechanism for inactivation of the D20N and D91N mutants by DHAP. It is proposed that both of these residues maintain the positive charge on the conserved lysine, 21. (b) The proposed reaction mechanism for the involvement of Asp 71 and Asp 101 in the catalyzed elimination of phosphate. (c) The possible hydrogen bonding schemes for the wild-type enzyme and the mutants D71N and D101N bound to the inhibitor 2PG.

dependent substrate inhibition of these enzymes, it is unlikely that either of these residues act as the catalytic base that abstracts the proton from the C-3 carbon.

Mutations that affect either the location or the charge associated with either D71 or D101 have a large effect on the turnover number, k_{cat} (Tables 5 and 6). However, since the endogenous *E. coli* methylglyoxal synthase gene was present in BL21(DE3) cells, a 5000-fold loss in mutant enzyme activity is indistinguishable from wild-type contamination (the approximate fold overexpression of the protein). This suggests that both residues are intimately involved with catalysis. Examination of the 2PG inhibition data is useful in formulating a hypothesis as to the role that each of these residues play in catalysis.

The activation caused by 2PG binding to the D71E mutant is reminiscent of 2PG activation of the phosphate-inhibited wild-type enzyme (Figure 6, panels c and d). This is unusual, especially considering that the mutant enzyme does not show any cooperativity in the presence or absence of phosphate. The displaced negative charge could take on the same role as the negatively charged phosphate and lock the enzyme into the "taut" state. It is also possible that the enzyme is in a different "taut" state unrelated to the phosphate-bound state, although this possibility seems unlikely. There is a 10-fold activation of D101E mutant by 2PG, and thus would seem to be a more extreme example of an enzyme locked into the "taut" state by the mutation (Figure 6, panels e and f). However, the fit suggests that K_i for 2PG is 3 orders of magnitude larger for the D71E mutant than the D101E mutant while the ratio L is only an order of magnitude larger than that for D71E (Table 7). This implies that "relaxed" D101E enzyme does not bind the ene-diol intermediate well.

The observation that two of the conserved aspartic acids are critical for catalysis is consistent with a proposed reaction mechanism that requires at least two general bases, one to abstract the proton from carbon C-3 and the other to abstract the proton from its hydroxyl group (Figure 7b). It is also possible that the two aspartic acid residues act in concert to abstract the C-3 proton. One aspartic acid abstracts the proton and the other provides an electrostatic environment to shift the pK_a of the first aspartic acid. Since triose phosphate isomerase is able to accomplish this task without

a second carboxylate to lower the pK_a of glutamic acid 165, this possibility is thought unlikely. Other critical roles in catalysis could include protonating the 2-hydroxyl of the ene-diolate or stabilizing the building of partial positive charge on the C1 carbon (next to the phosphate oxygen), but we do not consider these here.

The fact that the 2PG inhibits the D101N mutant uncompetitively suggests that 2PG is no longer binding to the substrate-binding form of the mutant. One interpretation of the data is that, during the catalytic cycle, the protonation state of the enzyme changes between binding substrate and binding product. By binding to the product binding form of the enzyme, 2PG would not compete with the substrate. The D101N mutant would be uncharged like the protonated wild-type enzyme after Asp 101 abstracts a proton from either Asp 71, the C-3 of DHAP, or the 3-hydroxyl of DHAP. However, if Asp 101 were to abstract a proton from C-3, then it would be expected that the D101N mutant would be able to bind 2PG as tightly or tighter than the wild-type enzyme. Further, the binding studies with the D101E mutant show that this mutant has a nearly normal K_d for DHAP, yet binds 2PG about 100-fold less tightly than the wild-type enzyme. Thus, the D101E mutant must have a distorted active site so that it is no longer able to stabilize the ene-diolate intermediate. These findings taken together are consistent with Asp 101 abstracting a proton from the 3-hydroxyl and the enzyme binding the substrate in a conformation where the 3 hydroxyl is on the same side of DHAP as the phosphate group.

The inhibitor 2PG is thought to mimic the ene-diolate intermediate in both methylglyoxal synthase and triose phosphate isomerase. In triosephosphate isomerase, the activity (k_{cat}/K_m) of the E165D mutant is 500-fold less than the wild-type, while inhibition constant for 2PG remains 20 μM for both the wild-type and E165D mutant (*23*). Thus, it might be expected that the catalytic base would not interact with the ene-diolate. However, the crystal structures of both the wild-type and E165D mutant show that the carboxylate of the inhibitor is within hydrogen-bonding distance of the catalytic base, 165 (*38, 40*). In methylglyoxal synthase, the activity of the D71N and D71E mutants is 1000-fold less than the wild-type, while the inhibition constant for 2PG remains nearly the same for the wild-type, D71N, and D71E mutants (Table 7 and Figures 5b and 6b). These results are consistent with a model where Asp 71 has the same role as Glu 165 in triosephosphate isomerase. On the basis of the kinetic behavior of the enzyme and these mutants in the presence of the inhibitor 2PG, a model of its binding the active site is shown in Figure 7c. This model is consistent with a mechanism in which Asp 71 abstracts the proton from the C-3 carbon of DHAP and Asp 101 abstracts the proton from the hydroxyl group or acts to change the pK_a of Asp 71 (Figure 7b).

The definitive roles for these four aspartic acid residues and the other "conserved" amino acid residues may be determined once the three-dimensional structure of methylglyoxal synthase is known. Of greater interest will be the mechanism by which phosphate allosterically controls this otherwise nonallosteric enzyme. The overexpression of large quantities of highly purified methylglyoxal synthase protein makes these studies possible.

ACKNOWLEDGMENT

We thank Dr. L. Mende-Mueller of *the Medical College of Wisconsin Protein and Nucleic Acid Core Facility* for the amino acid and amino-terminal peptide analyses. We especially thank Ms. Erika Pape and Mrs. Alison Holub for their patience and expert technical assistance.

REFERENCES

1. Murata, K., Fukuda, Y., Watanabe, K., Saikusa, T., Shimosaka, M., and Kimura, A. (1985) *Biochem. Biophys. Res. Commun. 131*, 190−198.
2. Ray, S., and Ray, M. (1981) *J. Biol. Chem. 256*, 6230−6233.
3. Thornalley, P. J. (1990) *Biochem. J. 269*, 1−11.
4. Cooper, R. A., and Anderson, A. (1970) *FEBS Lett. 11*, 273−276.
5. Cooper, R. A. (1984) *Annu. Rev. Microbiol. 44*, 812−826.
6. Fareleira, P., Legall, J., Xavier, A. V., and Santos, H. (1997) *J. Bacteriol. 179*, 3972−3980.
7. Rahman, A., Shahabuddin, and Hadi, S. M. (1990) *J. Biochem. Toxicol. 5*, 161−166.
8. Papoulis, A., al-Abed, Y., and Bucala, R. (1995) *Biochemistry 34*, 648−655.
9. Baskaran, S., and Balasubramanian, K. A. (1990) *Biochem. Int. 21*, 165−174.
10. Együd, L. G., and Szent-Györgyi, A. (1966) *Proc. Natl. Acad. U.S.A. 56*, 203−207.
11. Brownlee, M., and Cerami, A. (1981) *Annu. Rev. Biochem. 50*, 385−432.
12. Hopper, D. J., and Cooper, R. A. (1972) *Biochem. J. 128*, 321−329.
13. Cooper, R. A. (1974) *Eur. J. Biochem. 44*, 81−86.
14. Tsai, P., and Gracy, R. W. (1976) *J. Biol. Chem. 251*, 365−367.
15. Iyengar, R., and Rose, I. A. (1983) *J. Am. Chem. Soc. 105*, 3301−3303.
16. Murthy, N. S., Bakeris, T., Kavarana, M. J., Hamilton, D. S., Lan, Y., and Creighton, D. J. (1994) *J. Med. Chem. 37*, 2161−2166.
17. Summers, M. C., and Rose, I. A. (1977) *J. Am. Chem. Soc. 99*, 4475−4478.
18. Alber, T. C., Davenport, R. C., Jr., Giammona, D. A., Lolis, E., Petsko, G. A., and Ringe, D. (1987) *Cold Spring Harbor Symp. Quant. Biol. 52*, 603−613.
19. Joseph, D., Petsko, G. A., and Karplus, M. (1990) *Science 249*, 1425−1428.
20. Pompliano, D. L., Peyman, A., and Knowles, J. R. (1990) *Biochemistry 29*, 3186−3194.
21. Percy, D. S., and Harrison, D. H. T. (1996) *FASEB J. 10*, 1367.
22. Tötemeyer, S., Booth, N. A., Nichols, W. W., Dunbar, B., and Booth, I. R. (1998) *Mol. Microbiol. 27*, 553−562.
23. Straus, D., Raines, R., Kawashima, E., Knowles, J. R., and Gilbert, W. (1985) *Proc. Natl. Acad. Sci. U.S.A. 82*, 2272−2276.
24. Joseph-McCarthy, D., Rost, L. E., Komives, E. A., and Petsko, G. A. (1994) *Biochemistry 33*, 2824−2829.
25. Straub, A., and Effenberger, F. (1987) *Tetrahedron Lett. 28*, 1641−1644.
26. Bradford, M. (1976) *Anal. Biochem. 72*, 248−254.
27. Ornstein, L., and Davis, B. J. (1964) *Ann. N. Y. Acad. Sci. 121*, 321.
28. Ho, S. N., Hunt, H. D., Horton, R. M., Pullen, J. K., and Pease, L. R. (1989) *Gene 77*, 51−59.
29. Leatherbarrow, R. J. (1994) *GraFit: Data Analysis and Graphics Program*.
30. Segel, I. H. (1975) *Enzyme Kinetics: Behavior and Analysis of Rapid Equilibrium and Steady-State Enzyme Systems*, John Wiley and Sons, New York.
31. Hobohm, U., Houthaeve, T., and Sander, C. (1994) *Anal. Biochem. 222*, 202.

32. Pearson, W. R., and Lipman, D. J. (1988) *Proc. Natl. Acad. Sci. U.S.A. 85*, 2444−2448.
33. Wood, E. R., and Matson, S. W. (1989) *J. Biol. Chem. 264*, 8297−8303.
34. Blattner, F. R., Plunkett, G., III, Bloch, C. A., Perna, N. T., Burland, V., Riley, M., Collado-Vides, J., Glasner, J. D., Rode, C. K., Mayhew, G. F., Gregor, J., Davis, N. W., Kirkpatrick, H. A., Goeden, M. A., Rose, D. J., Mau, B., and Shao, Y. (1997) *Science 277*, 1453−1474.
35. Altschul, S. F., Gish, W., Miller, W., Myers, E. W., and Lipman, D. J. (1990) *J. Mol. Biol. 215*, 403−410.
36. Hopper, D. J., and Cooper, R. A. (1971) *FEBS Lett. 13*, 213-216.
37. Wolfenden, R. (1970) *Biochemistry 9*, 3404−3407.
38. Lolis, E., and Petsko, G. A. (1990) *Biochemistry 29*, 6619−6625.
39. Genetics Computer Group (GCG). (1982) *Wisconsin Package*.
40. Joseph-McCarthy, D., Petsko, G. A., and Karplus, M. (1995) *Protein Eng. 8*, 1103−1115.

BI980409P